Edelweiss Applied Science and Technology
ISSN: 2576-8484
Vol. 9, No. 9, 1471-1483
2025
Publisher: Learning Gate
DOI: 10.55214/2576-8484.v9i9.10155

Approximate solutions of transient reaction-diffusion equations for second-order regeneration at spherical microelectrodes via HPM

Rajendran Nalini[1], Athimoolam Meena[1*], Lakshmanan Rajendran[2], Mohammad Izadi[3]
[1]Department of Mathematics, Saraswathi Narayanan College, Madurai-625022, India; meensphd@gmail.com (A.M.),
[2]Department of Mathematics, AMET Deemed to be University, Kanathur, Chennai- 603112, India.
[3]Department of Applied Mathematics, Faculty of Mathematics and Computer, Shahid Bahonar University of Kerman, Kerman 76169-14111, Iran; izadi@uk.ac.ir (M.I.).

Abstract: The purpose of this study is to investigate the transient behavior of a second-order regeneration reaction at spherical microelectrodes, where nonlinear reaction–diffusion dynamics govern the system response. The research is designed to capture the interplay between electrochemical electron transfer and the subsequent homogeneous chemical reaction that regenerates the electroactive species, a process of considerable importance in electrochemical sensors and catalytic systems. The methodology combines analytical and numerical approaches: the homotopy perturbation method (HPM) is applied to derive approximate solutions for non-steady-state concentrations and current responses, while numerical simulations are carried out using Scilab to ensure accuracy and reliability. The approach effectively manages the inherent nonlinearity of the governing equations, offering tractable expressions for system behavior. The findings demonstrate strong agreement between the HPM-based analytical solutions and numerical simulations, confirming the validity of the proposed approach. The study concludes that HPM is a robust and efficient tool for analyzing nonlinear electrochemical systems. The practical implications highlight its potential application in the modeling and optimization of electrochemical devices, such as biosensors, microelectrodes, and catalytic fuel cells, where transient dynamics and regeneration mechanisms play a critical role.

Keywords: *Electrochemical modelling, Homotopy perturbation method, Reaction–diffusion equations, Second-order regeneration kinetics, Spherical microelectrodes.*

1. Introduction

Transient reaction–diffusion processes at spherical microelectrodes are fundamental to understanding complex electrochemical systems, particularly those involving second-order regeneration reactions. These reactions couple electron transfer with homogeneous chemical transformations, producing nonlinear behavior that influences both concentration profiles and current responses. The spherical geometry offers distinct advantages, such as radial symmetry and enhanced mass transport, making it an ideal platform for probing microscale kinetics. Modeling such systems requires solving nonlinear partial differential equations that capture spatial and temporal variations in concentration. Developing reliable analytical and numerical solutions to these equations is critical for advancing electrochemical theory. Moreover, these studies have wide practical applications in biosensing, electrocatalysis, and microanalytical chemistry, where accurate transient modeling supports improved device performance and optimization.

Electrode reaction mechanisms involving second-order homogeneous kinetics have been investigated using both numerical and analytical techniques. Molina and Laborda [1] proposed a generalized numerical scheme based on finite-difference equations to describe diffusion and kinetic processes across different time intervals. Eswari and Rajendran [2] applied the homotopy perturbation

History: Received: 9 July 2025; Revised: 19 August 2025; Accepted: 25 August 2025; Published: 23 September 2025
* Correspondence: meensphd@gmail.com

method (HPM) to derive approximate analytical expressions for concentration and current in homogeneous catalytic reactions at spherical microelectrodes. Molina, et al. [3] examined the chromate ampero metric behavior of CE processes at spherical microelectrodes under fast chemical conditions, while Delmastro [4] presented the polarographic kinetic current theory for second-order regeneration reactions. In addition, EC processes at ultramicroelectrodes have been extensively studied through computational simulations [5-7] and analytical approximations [8, 9]. Rajendran and co-workers further contributed by reporting accurate analytical solutions for steady-state chronoamperometric currents in EC reactions at disc [10] spheroidal ultramicroelectrodes. Izadi et al. applied numerical techniques to solve the nonlinear equation [11-13].

Despite these advances, accurate analytical approximations for transient concentrations and kinetic currents in second-order regeneration reactions at spherical electrodes remain unavailable. This gap limits predictive modeling of such nonlinear electrochemical systems under time-dependent conditions. To address this challenge, the present study employs the homotopy perturbation method (HPM) to obtain approximate analytical solutions for both concentration distributions and current responses. The approach not only manages the inherent nonlinearity of the governing equations but also provides results that can be compared with numerical simulations for validation. By bridging this gap, the study aims to extend the analytical toolkit available for modeling transient electrochemical processes at spherical electrodes.

2. Mathematical Formulation

The catalytic reaction scheme for second-order regeneration reaction at spherical electrodes can be written as follows:

$$O + ne \rightleftarrows R$$
$$2R \xrightarrow{k} O + Z$$

The reaction procedure for the second-order regeneration process is shown in Figure 1.

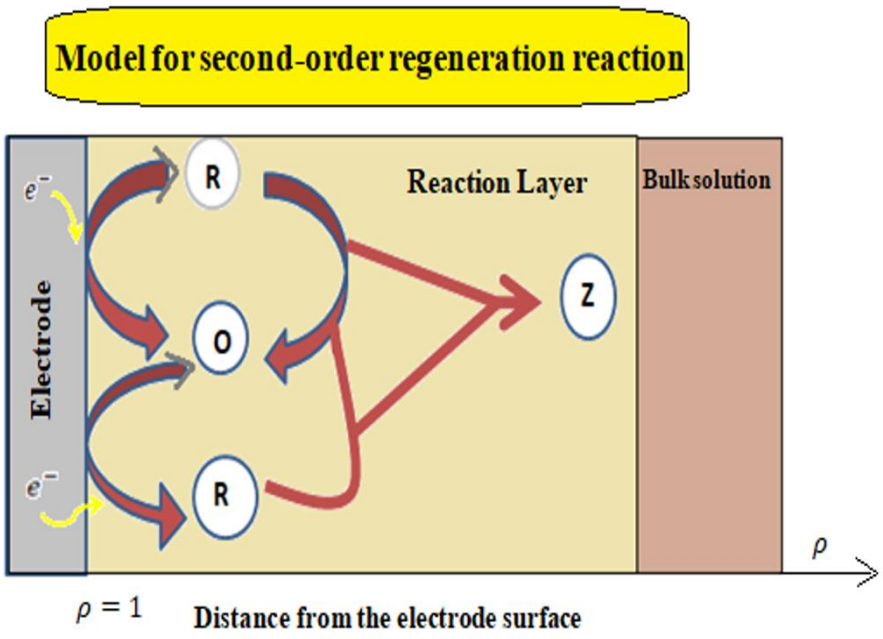

Figure 1.
The reaction scheme for second-order regeneration reaction.

Edelweiss Applied Science and Technology
ISSN: 2576-8484
Vol. 9, No. 9: 1471-1483, 2025
DOI: 10.55214/2576-8484.v9i9.10155

The nonlinear initial–boundary value problem describing a second-order regeneration reaction at spherical electrodes can be expressed in dimensional form as [4]:

$$\frac{\partial C_0(r,t)}{\partial t} = D_0\left[\frac{\partial^2 C_0(r,t)}{\partial r^2} + \frac{2}{r}\frac{\partial C_0(r,t)}{\partial r}\right] + \frac{k{C_R}^2(r,t)}{2}, \quad (1)$$

$$\frac{\partial C_R(r,t)}{\partial t} = D_R\left[\frac{\partial^2 C_R(r,t)}{\partial r^2} + \frac{2}{r}\frac{\partial C_R(r,t)}{\partial r}\right] - k{C_R}^2(r,t). \quad (2)$$

The corresponding initial and boundary conditions are:

$$\text{At } t = 0,\ r \geq r_o,\ C_0 = {C_0}^*, \text{ and } C_R = 0. \quad (3)$$

$$\text{At } r = r_o,\ C_0 = 0, \text{ and } D_0\frac{\partial C_0(r_o,t)}{\partial r} = -D_R\frac{\partial C_R(r_o,t)}{\partial r}. \quad (4)$$

$$\text{At } r = \infty,\ C_0 = {C_0}^*, \text{ and } C_R = 0. \quad (5)$$

The current is defined as:

$$\frac{i(t)}{nFA} = D_R\frac{\partial C_R(r_o,t)}{\partial r}. \quad (6)$$

Introducing the transformation $\psi(r,t) = 2C_0(r,t) + C_R(r,t)$ and assuming equal diffusion coefficients $D_0 = D_R = D$equations (1)–(2) reduce to:

$$\frac{\partial \psi(r,t)}{\partial t} = D\left[\frac{\partial^2 \psi(r,t)}{\partial r^2} + \frac{2}{r}\frac{\partial \psi(r,t)}{\partial r}\right], \quad (7)$$

$$\frac{\partial C_R(r,t)}{\partial t} = D\left[\frac{\partial^2 C_R(r,t)}{\partial r^2} + \frac{2}{r}\frac{\partial C_R(r,t)}{\partial r}\right] - k{C_R}^2(r,t). \quad (8)$$

The revised initial and boundary conditions become:

$$\text{At } t = 0,\ r \geq r_o,\ \psi(r,0) = 2{c_o}^*, \text{ and } C_R(r,0) = 0. \quad (9)$$

$$\text{At } r = r_o,\ \psi(r_o,t) = C_R(r_o,t), \text{ and } \frac{\partial \psi(r_o,t)}{\partial r} = -\frac{\partial C_R(r_o,t)}{\partial r}. \quad (10)$$

$$\text{At } r = \infty,\ \psi(\infty,t) = 2{c_o}^*, \text{ and } C_R(\infty,t) = 0. \quad (11)$$

The dimensional current expression becomes

$$\left[\frac{i(t)}{nFAD}\right] = \left[\frac{\partial C_R}{\partial r}\right]_{r=r_0}. \quad (12)$$

Introducing the dimensionless variables:

$$\rho = \frac{r}{r_o},\ T = \frac{Dt}{{r_o}^2},\ U = \frac{\psi}{2{c_o}^*},\ V = \frac{C_R}{2{c_o}^*},\ m = \frac{(2{c_o}^* k)(r_o)^2}{D}. \quad (13)$$

the governing equations (7)–(8) reduce to the following non-dimensional form:

$$\frac{\partial U(\rho,T)}{\partial T} = \frac{\partial^2 U(\rho,T)}{\partial \rho^2} + \frac{2}{\rho}\frac{\partial U(\rho,T)}{\partial \rho}, \quad (14)$$

$$\frac{\partial V(\rho,T)}{\partial T} = \frac{\partial^2 V(\rho,T)}{\partial \rho^2} + \frac{2}{\rho}\frac{\partial V(\rho,T)}{\partial \rho} - mV^2(\rho,T), \quad (15)$$

with initial and boundary conditions:

$$U(\rho,0) = 1,\ V(\rho,0) = 0. \quad (16)$$

$$U(1,T) = U(1,T) \text{and } U'(1,T) = -V'(1,T). \quad (17)$$

$$U(\infty,T) = 1,\ V(\infty,T) = 0. \quad (18)$$

Finally, the dimensionless current is expressed as:

$$\left[\frac{i(t)}{nFAD}\right] = \left[\frac{\partial V(\rho,T)}{\partial \rho}\right]_{\rho=1}. \quad (19)$$

The nonlinear reaction–diffusion equations modeling second-order regeneration at spherical microelectrodes have wide scientific and engineering applications. They aid in optimizing biosensors, simulating enzymatic processes in biofuel cells, guiding drug delivery system design, and improving electrochemical interfaces in batteries and super capacitors. This framework highlights the multidisciplinary importance of coupled diffusion–reaction dynamics near curved reactive surfaces.

Edelweiss Applied Science and Technology
ISSN: 2576-8484
Vol. 9, No. 9: 1471-1483, 2025
DOI: 10.55214/2576-8484.v9i9.10155

3. Result and Discussion

3.1. Solutions of Transient Concentrations and Current Via HPM

Numerous applied problems can be resolved by solving systems of nonlinear equations. However, significant progress has been made in developing accurate approximate analytical techniques over the last three decades. Among the most popular approaches are the variation iteration method [14], the hyperbolic and Pade approximation [15], the AGM method [16], the Adomian polynomials [17], and TSM method [18]. One of the popular techniques for resolving nonlinear differential equations is HPM [19, 20].

The HPM method was first proposed by He [21];He [22];He [23] and He [24]. Khan et al. applied the HPM method to solve the nonlinear boundary value problems [25, 26]. The nonlinear equation was also solved using the numerical scheme proposed by Srivastava and Izadi [27] and Izadi, et al. [13]. Recently, Rajendran and co-workers solved many nonlinear issues in physical and electrochemical sciences using the HPM method [28-35]. The approximate solutions for Eq. (14) and Eq. (15) using the homotopy perturbation approach are derived as follows (Appendix-A):

$$U(\rho,T) = 1 - \frac{1}{2\rho}\left(1 - erf\left(\frac{\rho-1}{2\sqrt{T}}\right)\right), \tag{20}$$

$$V(\rho,T) = \frac{1}{2\rho}\left(1 - erf\left(\frac{\rho-1}{2\sqrt{T}}\right)\right) + \frac{m\sqrt{T}}{\rho\sqrt{\pi}} - m\left(\frac{1}{\rho^2}\left(\frac{T}{4} + \frac{\sqrt{T}}{\sqrt{\pi}}\right)\right) + \frac{m}{4\rho}\left[\frac{(1-\rho)^2}{2} + T + \left(T + \frac{(1-\rho)^2}{2}\right)\left(erf\left(\frac{(1-\rho)}{2\sqrt{T}}\right)\right) + \frac{\sqrt{T}(1-\rho)e^{\frac{-(1-\rho)^2}{4T}}}{\sqrt{\pi}}\right]. \tag{21}$$

The nondimensional current takes the following form:

$$\mathrm{I}(T) = \left[\frac{i(t)}{nFAD}\right] = \left[\frac{\partial V(\rho,T)}{\partial \rho}\right]_{\rho=1} = \left|\left[\frac{mT}{4} + \frac{mT-1}{2\sqrt{T}\sqrt{\pi}} - \frac{1}{2}\right]\right|. \tag{22}$$

When m=0 we get

$$\mathrm{I}(T) = \left[\frac{i(t)}{nFAD}\right] = \left[\frac{\partial V(\rho,T)}{\partial \rho}\right]_{\rho=1} = \frac{1}{2}\left[1 + \frac{1}{\sqrt{\pi T}}\right]. \tag{23}$$

This expression describes the limiting diffusion current typically observed under semi-infinite spherical diffusion when a potential step is applied.

3.2. Validation of the Model

Numerical techniques are utilized to solve the nonlinear differential equations (14) and (15). This equation is solved using the SCILAB software pdex4 function, which resolves initial-boundary value issues for PDE. Table 1 and Tables 2a and 2b compare its numerical result with the HPM method of the dimensionless concentration of U and V for various values of dimensionless time T, respectively, for fixing the parameter value m. This Tables clearly shows that $U \approx 1$ and $V \approx 0$ when $T \geq 10$ and $\rho \geq 5$ and for higher values, the concentration approaches constant value, indicating that the species reaches equilibrium at higher spatial position. The dimensionless concentration values stabilize as T increases, which means that the system reaches a steady-state.

Edelweiss Applied Science and Technology
ISSN: 2576-8484
Vol. 9, No. 9: 1471-1483, 2025
DOI: 10.55214/2576-8484.v9i9.10155

Table 1.
Comparing the analytical and numerical results for U(ρ,T) for different values of time T.

	Concentration of U(ρ, T)														
	T=0.1			T=1			T=3			T=5			T=10		
ρ	Numerial	Analytical RJM Eq. (20)	Deviation	Numerical	Analytical RJM Eq. (20)	Deviation	Numerical	Analytical RJM Eq. (20)	Deviation	Numerical	Analytical RJM Eq. (20)	Deviation	Numerical	Analytical RJM Eq. (20)	Deviation
1	0.5000	0.5000	0.0000	0.5000	0.5000	0.0000	0.5000	0.5000	0.0000	0.5000	0.5000	0.0000	0.5000	0.5000	0.0000
2	0.9932	0.9937	0.0005	0.8796	0.8801	0.0005	0.8289	0.8292	0.0003	0.8123	0.8120	0.0003	0.7943	0.7942	0.0001
3	1.0000	0.9999	0.0001	0.9734	0.9738	0.0004	0.9306	0.9301	0.0005	0.9125	0.9122	0.0003	0.8909	0.8909	0.0000
4	1.0000	1.0000	0.0000	0.9956	0.9958	0.0002	0.9721	0.9724	0.0003	0.9575	0.9572	0.0003	0.9373	0.9372	0.0001
5	1.0000	1.0000	0.0000	0.9995	0.9995	0.0000	0.9896	0.9898	0.0002	0.9796	0.9794	0.0002	0.9631	0.9629	0.0002
6	1.0000	1.0000	0.0000	1.0000	0.9999	0.0001	0.9965	0.9966	0.0001	0.9907	0.9905	0.0002	0.9783	0.9780	0.0003
7	1.0000	1.0000	0.0000	1.0000	0.9999	0.0001	0.9989	0.9989	0.0000	0.9960	0.9959	0.0001	0.9877	0.9872	0.0005
8	1.0000	1.0000	0.0000	1.0000	0.9999	0.0001	0.9997	0.9997	0.0000	0.9984	0.9983	0.0001	0.9935	0.9927	0.0008
9	1.0000	1.0000	0.0000	1.0000	0.9999	0.0001	0.9999	0.9999	0.0000	0.9995	0.9994	0.0001	0.9973	0.9959	0.0014
10	1.0000	1.0000	0.0000	1.0000	1.0000	0.0000	1.0000	0.9999	0.0001	1.0000	0.9998	0.0002	1.0000	0.9978	0.0022
Average Deviation			0.0001	Average Deviation		0.0001	Average Deviation		0.0002	Average Deviation		0.0002	Average Deviation		0.0006

Table 2a.
Comparing the analytical and numerical concentration of specie V(ρ,T) for different values of time T and for a fixed value of m=0.1.

	Concentration of V(ρ, T) (m = 0.1)														
	T=0.1			T=1			T=3			T=5			T=10		
ρ	Numerical	Analytical RJM Eq. (21)	Deviation	Numerical	Analytical RJM Eq. (21)	Deviation	Numerical	Analytical RJM Eq. (21)	Deviation	Numerical	Analytical RJM Eq. (21)	Deviation	Numerical	Analytical RJM Eq. (21)	Deviation
1	0.5000	0.5000	0.0000	0.5000	0.5000	0.0000	0.5000	0.5000	0.0000	0.5000	0.5000	0.0000	0.5000	0.5000	0.0000
2	0.0068	0.0102	0.0034	0.1196	0.1312	0.0116	0.1689	0.1951	0.0262	0.1845	0.2249	0.0404	0.2010	0.2742	0.0732
3	0.0000	0.0037	0.0037	0.0264	0.0365	0.0101	0.0684	0.0880	0.0196	0.0856	0.1155	0.0299	0.1055	0.1596	0.0541
4	0.0000	0.0032	0.0032	0.0043	0.0133	0.0090	0.0275	0.0429	0.0154	0.0416	0.0639	0.0223	0.0605	0.0994	0.0389
5	0.0000	0.0028	0.0028	0.0005	0.0085	0.0080	0.0103	0.0234	0.0131	0.0191	0.0378	0.0187	0.0356	0.0651	0.0295
6	0.0000	0.0024	0.0024	0.0000	0.0072	0.0072	0.0035	0.0151	0.0116	0.0092	0.0243	0.0151	0.0209	0.0446	0.0237
7	0.0000	0.0021	0.0021	0.0000	0.0064	0.0064	0.0011	0.0115	0.0104	0.0031	0.0173	0.0142	0.0119	0.0320	0.0201
8	0.0000	0.0019	0.0019	0.0000	0.0058	0.0058	0.0003	0.0098	0.0095	0.0016	0.0136	0.0120	0.0063	0.0242	0.0179
9	0.0000	0.0017	0.0017	0.0000	0.0053	0.0053	0.0000	0.0088	0.0088	0.0005	0.0116	0.0111	0.0026	0.0192	0.0166
10	0.0000	0.0016	0.0016	0.0000	0.0048	0.0048	0.0000	0.0081	0.0081	0.0000	0.0103	0.0103	0.0000	0.0161	0.0161
Average Deviation			0.0023	Average Deviation		0.0068	Average Deviation		0.0123	Average Deviation		0.0174	Average Deviation		0.0290

Edelweiss Applied Science and Technology
ISSN: 2576-8484
Vol. 9, No. 9: 1471-1483, 2025
DOI: 10.55214/2576-8484.v9i9.10155

Table 2b.
Comparing the analytical and numerical concentration of specie $V(\rho,T)$ for different values of time T and for a fixed value of m=0.01.

Concentration of V(ρ,T) (m = 0.01)																
	T=0.1			**T=1**			**T=3**			**T=5**			**T=10**			
ρ	**Numerical**	**Analytical RJM Eq. (21)**	**Deviation**	**Numerical**	**Analytical RJM Eq. (21)**	**Deviation**	**Numerical**	**Analytical RJM Eq. (21)**	**Deviation**	**Numerical**	**Analytical RJM Eq. (21)**	**Deviation**	**Numerical**	**Analytical RJM Eq. (21)**	**Deviation**
1	0.5000	0.5000	0.0000	0.5000	0.5000	0.0000	0.5000	0.5000	0.0000	0.5000	0.5000	0.0000	0.5000	0.5000	0.0000
2	0.0067	0.0067	0.0000	0.1203	0.1210	0.0007	0.1709	0.1732	0.0023	0.1873	0.1917	0.0044	0.2052	0.2126	0.0074
3	0.0000	0.0004	0.0004	0.0267	0.0272	0.0005	0.0693	0.0709	0.0016	0.0873	0.0906	0.0033	0.1087	0.1142	0.0055
4	0.0000	0.0003	0.0003	0.0044	0.0051	0.0007	0.0278	0.0291	0.0013	0.0425	0.0449	0.0024	0.0625	0.0665	0.0040
5	0.0000	0.0003	0.0003	0.0005	0.0013	0.0008	0.0104	0.0116	0.0012	0.0203	0.0223	0.0020	0.0368	0.0399	0.0031
6	0.0000	0.0002	0.0002	0.0000	0.0008	0.0008	0.0035	0.0046	0.0011	0.0093	0.0109	0.0016	0.0216	0.0242	0.0026
7	0.0000	0.0002	0.0002	0.0000	0.0006	0.0006	0.0011	0.0021	0.0010	0.0040	0.0054	0.0014	0.0123	0.0148	0.0025
8	0.0000	0.0002	0.0002	0.0000	0.0006	0.0006	0.0003	0.0012	0.0009	0.0016	0.0029	0.0013	0.0065	0.0090	0.0025
9	0.0000	0.0002	0.0002	0.0000	0.0005	0.0005	0.0000	0.0009	0.0009	0.0005	0.0017	0.0012	0.0028	0.0056	0.0028
10	0.0000	0.0001	0.0001	0.0000	0.0005	0.0005	0.0000	0.0008	0.0008	0.0000	0.0012	0.0012	0.0000	0.0036	0.0036
Average Deviation			0.0002	Average Deviation		0.0006	Average Deviation		0.0011	Average Deviation		0.0019	Average Deviation		0.0034

Edelweiss Applied Science and Technology
ISSN: 2576-8484
Vol. 9, No. 9: 1471-1483, 2025
DOI: 10.55214/2576-8484.v9i9.10155

3.3. Parametric Analysis of Concentration and Current

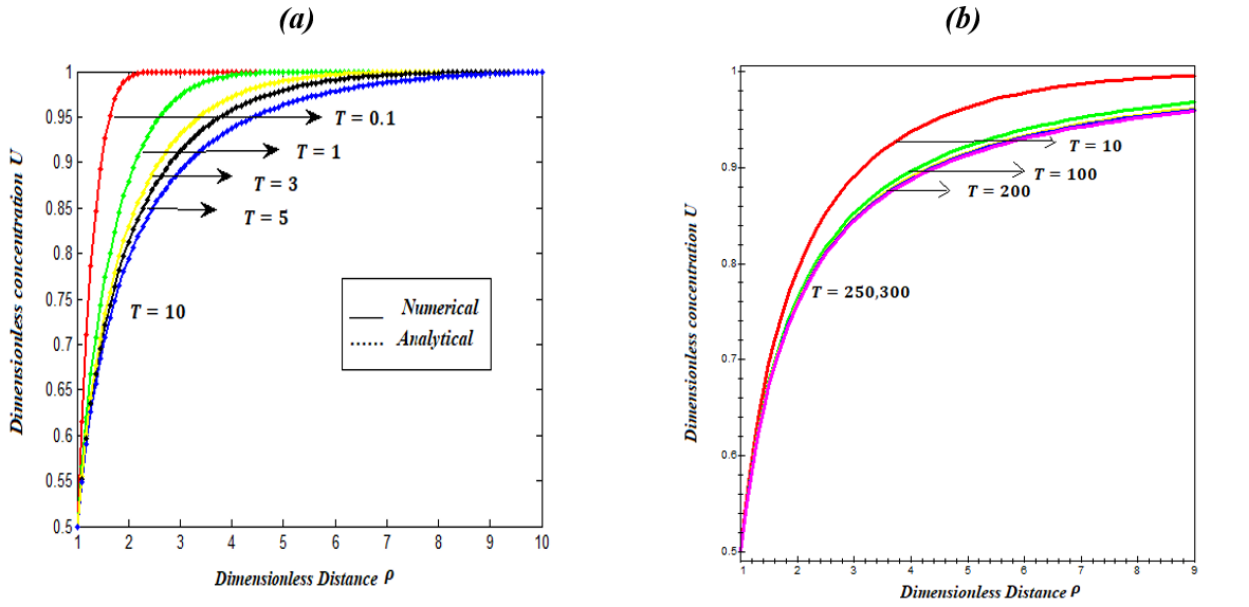

Figure 2.
(a,b). (a). Comparison of dimensionless concentration U were calculated using Eq. (14) and Eq. (20). (b) shows the steady state of dimensionless concentration U.

In Figure 2(a) at small time the concentration rapidly increases with distance, reaching a nearly steady-state. As T increases (i.e. $T = 1,3,5,10$), the concentration profile smoothens and extends further into the domain. Also, clear that as time increases, the concentration value rises and concentration value is the same (i.e. $U = 1$) when $\rho \geq 10$ for all values of time T. The system appears to describe a diffusion-like process where concentration gradually reaches equilibrium. The boundary conditions likely enforce a high concentration when $2 \leq \rho \leq 4$ and also Fig. 2(b) shows the steady-state concentration U at $T \geq 100$.From the equation (20) and Fig.2(a,b) it is observed that the concentration of U is minimum at ρ =1 and minimum value is 0.5.The concentration of U has been estimated to be maximal when ρ = 10, with a peak value of one.

Edelweiss Applied Science and Technology
ISSN: 2576-8484
Vol. 9, No. 9: 1471-1483, 2025
DOI: 10.55214/2576-8484.v9i9.10155

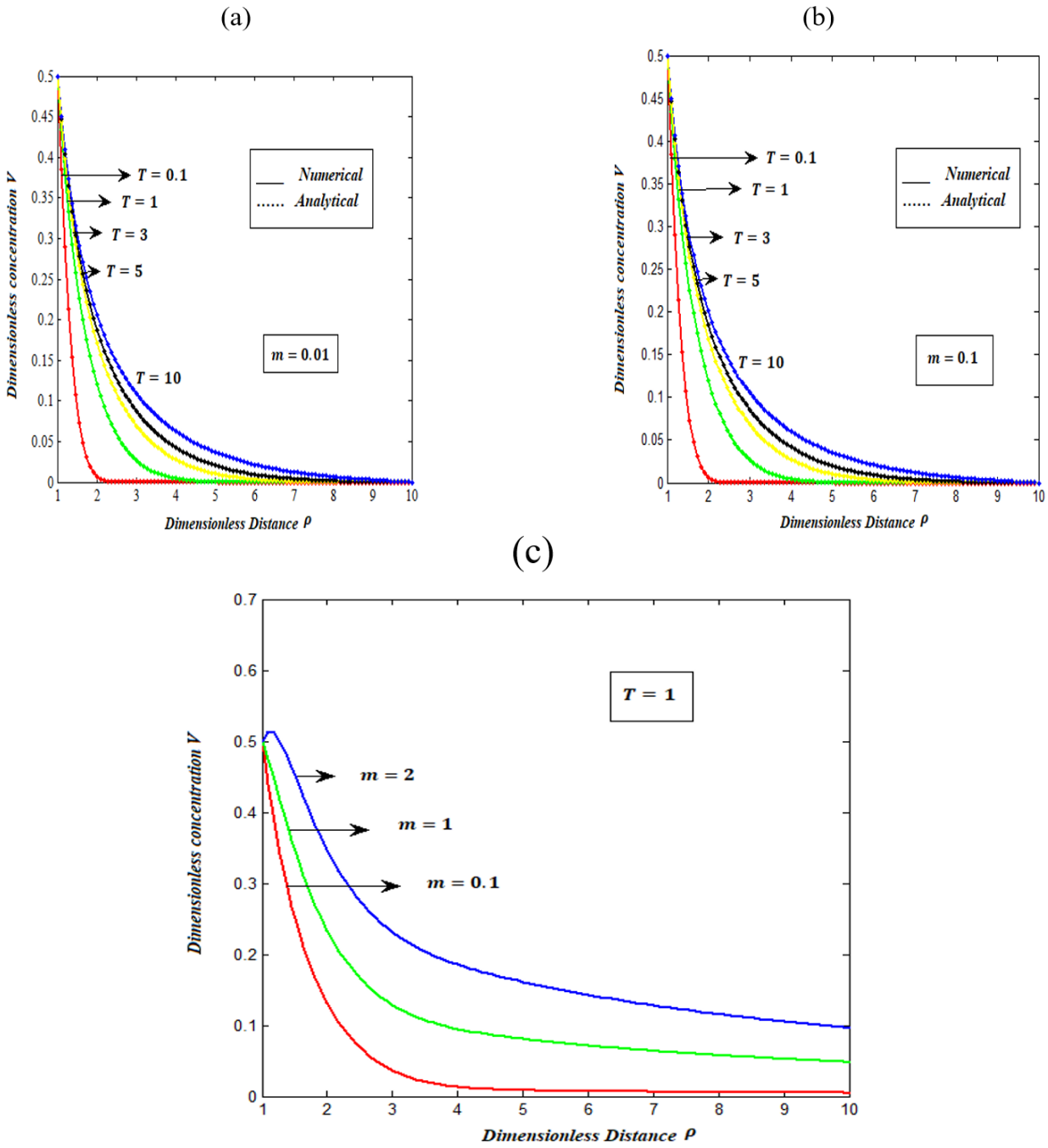

Figure 3.
(a-c) Comparison of concentration V using Eq. (15) for various values of T (a) when $m = 0.1$ (b) when $m = 0.01$ (c) various values of m (dimensionless parameter).

In Figure 3(a) and 3(b) plots the $V(\rho, T)$ for a range of distance ρ for various value of dimensionless time $T$when parameter $m = 0.1$ and $m = 0.01$respectively. Here the value of $V(\rho, T)$ is high when T increases and its value is equal (i.e. $V = 0$) for all values of time T at $\rho \geq 10$. If larger m $(m = 0.1)$ leads to a slower concentration decay while smaller m $(m = 0.01)$ results in a more rapid drop in

Edelweiss Applied Science and Technology
ISSN: 2576-8484
Vol. 9, No. 9: 1471-1483, 2025
DOI: 10.55214/2576-8484.v9i9.10155

concentration. According to equation (21) and figure 2(*a*,*b*), the concentration of V reaches its maximum at ρ=0 and reaches its maximum value of 0.5.

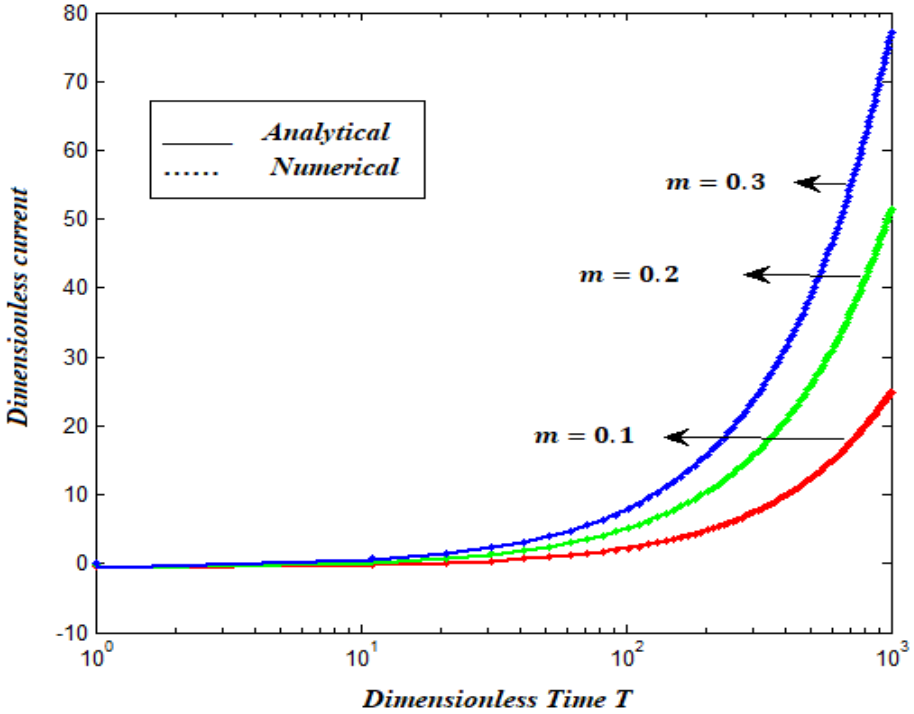

Figure 4.
Dimensionless current were calculated using Eq. (22) for the various values of parameter m.

Figure 4 represents the variation of current over time T for various values of m. The dimensionless current starts from a lower value and increases as time progresses. As T increases, the system becomes more stable, causing the current to change. A higher m likely means faster transport or diffusion, leading to a more pronounced increase in current. A comparison between the analytical and simulation results for different values of m is provided in Table 3. The highest deviation between the analytical predictions and numerical simulations, observed across Tables 1 to 3, is 0.4071.

Table 3.
Comparison of the analytical results of the current with simulation result.

Dimensionless current I									
T	**m=0.1**			**m=0.5**			**m=1**		
	Numerical	**Analytical RJM Eq. (22)**	**Deviation**	**Numerical**	**Analytical RJM Eq. (22)**	**Deviation**	**Numerical**	**Analytical RJM Eq. (22)**	**Deviation**
5	0.0004	0.0002	0.0002	0.8299	0.3143	0.5156	2.2199	1.2548	0.9651
10	0.0073	0.0051	0.0022	1.4792	1.1069	0.3723	3.5194	2.8031	0.7163
20	0.0997	0.0631	0.0366	2.7788	2.5678	0.2110	6.1178	5.6988	0.4190
30	0.3594	0.3530	0.0064	4.0775	3.9712	0.1063	8.7151	8.4940	0.2211
40	0.6189	0.6338	0.0149	5.3755	5.3477	0.0278	11.3113	11.2391	0.0722
50	0.8783	0.9096	0.0313	6.6730	6.7077	0.0347	13.9065	13.9553	0.0488
Average Deviation			0.0153	Average Deviation		0.2113	Average Deviation		0.4071

Edelweiss Applied Science and Technology
ISSN: 2576-8484
Vol. 9, No. 9: 1471-1483, 2025
DOI: 10.55214/2576-8484.v9i9.10155

4. Future Scope

The homotopy perturbation method (HPM) offers a powerful framework for obtaining accurate analytical approximations to nonlinear boundary value problems with minimal computational effort. Its versatility extends to second-order homogeneous kinetics [36] and biological wave phenomena [37]. Similar nonlinear initial–boundary value problems arise in diverse fields, including heat propagation in absorptive media, thermal energy transfer in plasmas, and dead-core formation processes [38]. The efficiency of HPM in simplifying nonlinear systems makes it particularly valuable for real-time simulations and for bridging empirical models with theoretical frameworks, thereby advancing applications across science and engineering.

5. Conclusion

This study developed and analyzed nonlinear transient reaction–diffusion equations describing a second-order regeneration process at spherical microelectrodes with equal diffusion coefficients. Using the homotopy perturbation method (HPM), convergent analytical solutions were obtained, effectively capturing nonlinear dynamics under transient conditions. The method successfully addressed nonlinearities from second-order kinetics and Butler–Volmer type boundary conditions, proving robust for curved geometries. These approximations provide insights into concentration profiles and fluxes, reducing dependence on numerical simulations. Beyond theory, the approach offers practical implications for optimizing biosensors, enzymatic biofuel cells, and electrochemical energy devices, where accurate modeling of coupled diffusion–reaction processes is crucial for performance improvement.

Transparency:

The authors confirm that the manuscript is an honest, accurate, and transparent account of the study; that no vital features of the study have been omitted; and that any discrepancies from the study as planned have been explained. This study followed all ethical practices during writing.

Copyright:

References

[1] A. Molina and E. Laborda, "Detailed theoretical treatment of homogeneous chemical reactions coupled to interfacial charge transfers," *Electrochimica Acta*, vol. 286, pp. 374-396, 2018. https://doi.org/10.1016/j.electacta.2018.07.142

[2] A. Eswari and L. Rajendran, "Analytical expressions of concentration and current in homogeneous catalytic reactions at spherical microelectrodes: Homotopy perturbation approach," *Journal of Electroanalytical Chemistry*, no. 651, p. 173-184, 2011.

[3] Á. Molina, I. Morales, and M. López-Tenés, "Chronoamperometric behaviour of a CE process with fast chemical reactions at spherical electrodes and microelectrodes. Comparison with a catalytic reaction," *Electrochemistry communications*, vol. 8, no. 6, pp. 1062-1070, 2006.

[4] J. R. Delmastro, "Theory of polarographic kinetic currents for second-order regeneration reactions at spherical electrodes. II. Numerical solution of the integral equations for steady-state behavior," *Analytical Chemistry*, vol. 41, no. 6, pp. 747-753, 1969.

[5] J. Galceran, J. Puy, J. Salvador, J. Cecília, and H. P. van Leeuwen, "Voltammetric lability of metal complexes at spherical microelectrodes with various radii," *Journal of Electroanalytical Chemistry*, vol. 505, no. 1-2, pp. 85-94, 2001.

[6] L. Bieniasz and D. Britz, "Recent developments in digital simulation of electroanalytical experiments," *Polish Journal of Chemistry*, vol. 78, no. 9, pp. 1195-1219, 2004.

[7] D. Britz, *Digital simulation in electrochemistry*. Berlin, Germany: Springer, 2005.

[8] Á. Molina and I. Morales, "Singularities of the catalytic mechanism in its route to the steady state," *Journal of Electroanalytical Chemistry*, vol. 583, no. 2, pp. 193-202, 2005.

[9] J. Galceran, S. Taylor, and P. Bartlett, "Modelling the steady-state current at the inlaid disc microelectrode for homogeneous mediated enzyme catalysed reactions," *Journal of Electroanalytical Chemistry*, vol. 506, no. 2, pp. 65-81, 2001.

[10] L. Rajendran, "Analytical solution for the steady-state chronoamperometric current for an ec′ reaction at spheroidal ultramicroelectrodes," *Journal of Theoretical and Computational Chemistry*, vol. 5, no. 01, pp. 11-24, 2006.
[11] M. Izadi, S. K. Yadav, and G. Methi, "Two efficient numerical techniques for solutions of fractional shallow water equation," *Partial Differential Equations in Applied Mathematics*, vol. 9, p. 100619, 2024.
[12] M. Izadi, "Numerical approximation of Hunter-Saxton equation by an efficient accurate approach on long time domains," *UPB Sci. Bull. Ser. A*, vol. 83, no. 1, pp. 291-300, 2021.
[13] M. Izadi, H. M. Srivastava, and W. Adel, "The nonlinear reactive transport model: An efficient approximation method based on quasilinearization and Bessel matrix method," *Applied and Computational Mathematics*, vol. 23, no. 2, pp. 135-158, 2024.
[14] J.-H. He, "Variational iteration method–a kind of non-linear analytical technique: some examples," *International Journal of Non-Linear Mechanics*, vol. 34, no. 4, pp. 699-708, 1999.
[15] K. Nirmala, B. Manimegalai, and L. Rajendran, "Steady-State substrate and product concentrations for non-michaelis-menten kinetics in an amperometric biosensor–hyperbolic function and padéapproximants method," *International Journal of Electrochemical Science*, vol. 15, no. 6, pp. 5682-5697, 2020.
[16] M. E. Lyons, "Transport and kinetics in electrocatalytic thin film biosensors:Bounded diffusion with non-Michaelis-Menten reaction kinetics," *Journal of Solid State Electrochemistry*, vol. 24, no. 11, pp. 2751-2761, 2020.
[17] Y. Khan, H. Vazquez-Leal, and N. Faraz, "An auxiliary parameter method using adomian polynomials and laplace transformation for nonlinear differential equations," *Applied Mathematical Modelling*, vol. 37, no. 5, pp. 2702-2708, 2013.
[18] R. Usha and L. Rajendran, "Taylor's series method for solving the nonlinear reaction-diffusion equation in the electroactive polymer film," *Chemical Physics Letters*, vol. 754, p. 137573, 2020.
[19] J.-H. He, "Homotopy perturbation method with an auxiliary term," in *Abstract and Applied Analysis*, 2012: Wiley Online Library.
[20] J.-H. He, "A coupling method of a homotopy technique and a perturbation technique for non-linear problems," *International Journal of Non-Linear Mechanics*, vol. 35, no. 1, pp. 37-43, 2000.
[21] J.-H. He, "Homotopy perturbation technique," *Computer Methods in Applied Mechanics and Engineering*, vol. 178, no. 3-4, pp. 257-262, 1999.
[22] J.-H. He, "Homotopy perturbation method: A new nonlinear analytical technique," *Applied Mathematics and computation*, vol. 135, no. 1, pp. 73-79, 2003.
[23] J.-H. He, "The homotopy perturbation method for nonlinear oscillators with discontinuities," *Applied Mathematics and Computation*, vol. 151, no. 1, pp. 287-292, 2004.
[24] J.-H. He, "Homotopy perturbation method for bifurcation of nonlinear problems," *International Journal of Nonlinear Sciences and Numerical Simulation*, vol. 6, no. 2, pp. 207-208, 2005.
[25] Y. Khan and Q. Wu, "Homotopy perturbation transform method for nonlinear equations using He's polynomials," *Computers & Mathematics with Applications*, vol. 61, no. 8, pp. 1963-1967, 2011.
[26] Y. Khan and M. Usman, "Modified homotopy perturbation transform method: A paradigm for nonlinear boundary layer problems," *International Journal of Nonlinear Sciences and Numerical Simulation*, vol. 15, no. 1, pp. 19-25, 2014.
[27] H. M. Srivastava and M. Izadi, "The Rothe-Newton approach to simulate the variable coefficient convection-diffusion equations," *Journal of Mahani Mathematical Research*, vol. 11, no. 2, pp. 141-158, 2022.
[28] L. Rajendran, R. Swaminathan, and M. C. Devi, *A closer look of nonlinear reaction-diffusion equations*. New York, NY: Nova Science Publishers, 2020.
[29] M. Chitra Devi, P. Pirabaharan, L. Rajendran, and M. Abukhaled, "Amperometric biosensors in an uncompetitive inhibition processes: A complete theoretical and numerical analysis," *Reaction Kinetics, Mechanisms and Catalysis*, vol. 133, no. 2, pp. 655-668, 2021.
[30] R. Swaminathan, M. C. Devi, L. Rajendran, and K. Venugopal, "Sensitivity and resistance of amperometric biosensors in substrate inhibition processes," *Journal of Electroanalytical Chemistry*, vol. 895, p. 115527, 2021.
[31] B. Manimegalai, M. E. Lyons, and L. Rajendran, "Transient chronoamperometric current at rotating disc electrode for second-order ECE reactions," *Journal of Electroanalytical Chemistry*, vol. 902, p. 115775, 2021.
[32] R. J. Salomi, S. V. Sylvia, L. Rajendran, and M. Lyons, "Transient current, sensitivity and resistance of biosensors acting in a trigger mode: Theoretical study," *Journal of Electroanalytical Chemistry*, vol. 895, p. 115421, 2021.
[33] B. Manimegalai, L. Rajendran, and M. Lyons, "Theory of the transient current response for the homogeneous mediated enzyme catalytic mechanism at the rotating disc electrode," *International Journal of Electrochemical Science*, vol. 16, no. 9, p. 210946, 2021.
[34] S. V. Sylvia, R. J. Salomi, L. Rajendran, and M. Lyons, "Amperometric biosensors and coupled enzyme nonlinear reactions processes: A complete theoretical and numerical approach," *Electrochimica Acta*, vol. 415, p. 140236, 2022.
[35] S. V. Sylvia, R. J. Salomi, M. Lyons, and L. Rajendran, "Transient current of catalytic processes at chemically modified electrodes," *International Journal of Electrochemical Science*, vol. 16, no. 4, p. 210452, 2021.
[36] R. G. Compton, "Understanding voltammetry," 2nd ed. ed. Singapore: World Scientific Publishing, 2010, p. 138.
[37] J. D. Murray, *Mathematical biology: I. An introduction* 3rd ed. ed. New York: Springer, 2002.

Edelweiss Applied Science and Technology
ISSN: 2576-8484
Vol. 9, No. 9: 1471-1483, 2025
DOI: 10.55214/2576-8484.v9i9.10155

[38] P. Zheng, C. Mu, and X. Hu, "Dead-core rate for the fast diffusion equation with strong absorption in higher dimensional cases," *Applied Mathematics and Computation*, vol. 335, pp. 292-304, 2018.

Appendix A.

Solution of equations (14) and (15).

The equations (14) and (15) can be written as follows:

$$\frac{\partial^2 U}{\partial \rho^2}+\frac{2}{\rho}\frac{\partial U}{\partial \rho}-\frac{\partial U}{\partial T}=0, \tag{A1}$$

$$\frac{\partial^2 V}{\partial \rho^2}+\frac{2}{\rho}\frac{\partial V}{\partial \rho}-\frac{\partial V}{\partial T}-mV^2=0. \tag{A2}$$

Dimensionless initial and boundary conditions are as follows:

$$\text{At } T=0,\ U=1,\ V=0. \tag{A3}$$

$$\text{At } \rho=1,\ U=V, \text{ and } U'=-V'. \tag{A4}$$

$$\text{At } \rho=\infty,\quad U(\infty)=1,\quad V(\infty)=0. \tag{A5}$$

The homotopy for the nonlinear equation (A2) can be constructed as follows:

$$(1-p)\left[\frac{\partial^2 V}{\partial \rho^2}+\frac{2}{\rho}\frac{\partial V}{\partial \rho}-\frac{\partial V}{\partial T}\right]+p\left[\frac{\partial^2 V}{\partial \rho^2}+\frac{2}{\rho}\frac{\partial V}{\partial \rho}-\frac{\partial V}{\partial T}-mV^2\right]=0. \tag{A6}$$

Now assume that the solution of Eqn.(A2) is

$$V=V_0+pV_1+p^2V_2+\cdots. \tag{A7}$$

By inserting Eq. (A7) into Eq. (A6) and matching powers of p, the following equations are obtained.

$$p^0:\frac{\partial^2 V_0}{\partial \rho^2}+\frac{2}{\rho}\frac{\partial V_0}{\partial \rho}-\frac{\partial V_0}{\partial T}=0, \tag{A8}$$

$$p^1:\frac{\partial^2 V_1}{\partial \rho^2}+\frac{2}{\rho}\frac{\partial V_1}{\partial \rho}-\frac{\partial V_1}{\partial T}-m{V_0}^2=0. \tag{A9}$$

The conditions for (A8) are as follows:

$$T=0,\ U=1,\ V_0=0, \tag{A10}$$

$$\rho=1,\ U(1)=V_0(1),\quad U'(1)=-{V_0}'(1), \tag{A11}$$

$$\rho=\infty,\ U(\infty)=1,\ V_0(\infty)=0. \tag{A12}$$

The following are dimensionless conditions for (A9):

$$T=0,\ V_1=0, \tag{A13}$$

$$\rho=1,\quad V_1(1)=0,\quad {V_1}'(1)=0, \tag{A14}$$

$$\rho=\infty,\quad V_1(\infty)=0. \tag{A15}$$

Taking Laplace transformation with respect to T to the Eqs. (A1) and (A8) we get

Edelweiss Applied Science and Technology
ISSN: 2576-8484
Vol. 9, No. 9: 1471-1483, 2025
DOI: 10.55214/2576-8484.v9i9.10155

$$\frac{\partial^2 \overline{U}}{\partial \rho^2} + \frac{2}{\rho}\frac{\partial \overline{U}}{\partial \rho} - s\overline{U} + 1 = 0, \tag{A16}$$

$$\frac{\partial^2 \overline{V_0}}{\partial \rho^2} + \frac{2}{\rho}\frac{\partial \overline{V_0}}{\partial \rho} - s\overline{V_0} = 0, \tag{A17}$$

where s is the Laplace variable and the over bar signifies a quantity that has undergone Laplace transformation. On solving Eqs. (A16) and (A17) with the initial and boundary conditions,we get the following results.

$$\overline{U}(\rho, s) = \frac{1}{s} - \frac{e^{-\rho\sqrt{s}}}{2\rho s e^{-\sqrt{s}}}, \tag{A18}$$

$$\overline{V_0}(\rho, s) = \frac{e^{-\rho\sqrt{s}}}{2\rho s e^{-\sqrt{s}}}. \tag{A19}$$

Using inverse Laplace transform, the final results can be obtained as follows:

$$U(\rho, T) = 1 - \frac{1}{2\rho}\left(1 - erf\left(\frac{\rho-1}{2\sqrt{T}}\right)\right), \tag{A20}$$

$$V_0(\rho, T) = \frac{1}{2\rho}\left(1 - erf\left(\frac{\rho-1}{2\sqrt{T}}\right)\right). \tag{A21}$$

Taking Laplace transformation with respect to T to the Eqs. (A9) we get

$$\frac{\partial^2 \overline{V_1}}{\partial \rho^2} + \frac{2}{\rho}\frac{\partial \overline{V_1}}{\partial \rho} - s\overline{V_1} - \frac{m}{4\rho^2}\left(\frac{1}{s} - \frac{2(\rho-1)}{\sqrt{s}}\right) = 0. \tag{A22}$$

On solving Eqs. (A22) using reduction of order , we get the following results.

$$\overline{V_1}(\rho, S) = \frac{m e^{\sqrt{s}(1-\rho)}}{4s^2\rho} + \frac{m}{2\rho s^{\frac{3}{2}}} - \frac{m(1+2\sqrt{s})}{4s^2}(\rho^{-2} + \frac{2\rho^{-4}}{s} + \frac{24\rho^{-6}}{s^2} + \cdots) \approx \frac{m e^{\sqrt{s}(1-\rho)}}{4s^2\rho} + \frac{m}{2\rho s^{\frac{3}{2}}} - \frac{m(1+2\sqrt{s})}{4s^2}(\rho^{-2}). \tag{A23}$$

Using inverse Laplace transform, the final results can be obtained as follows:

$$V_1(\rho, T) = \frac{m}{4\rho}\left[\left(T + \frac{(1-\rho)^2}{2}\right)\left(erf\left(\frac{(1-\rho)}{2\sqrt{T}}\right)\right) + \frac{\sqrt{T}(1-\rho)e^{\frac{-(1-\rho)^2}{4T}}}{\sqrt{\pi}} + \frac{(1-\rho)^2}{2} + T\right] + \frac{m\sqrt{T}}{\rho\sqrt{\pi}} - m\left(\frac{1}{\rho^2}\left(\frac{T}{4} + \frac{\sqrt{T}}{\sqrt{\pi}}\right)\right). \tag{A24}$$

According to the analysis using HPM, we find that.

$$U(\rho, T) = 1 - \frac{1}{2\rho}\left(1 - erf\left(\frac{\rho-1}{2\sqrt{T}}\right)\right), \tag{A25}$$

$$V(\rho, T) = \lim_{p\to 1} V(\rho) \approx V_0 + V_1$$

$$\approx \frac{1}{2\rho}\left(1 - erf\left(\frac{\rho-1}{2\sqrt{T}}\right)\right) + \frac{m}{4\rho}\left[\left(T + \frac{(1-\rho)^2}{2}\right)\left(erf\left(\frac{(1-\rho)}{2\sqrt{T}}\right)\right) + \frac{\sqrt{T}(1-\rho)e^{\frac{-(1-\rho)^2}{4T}}}{\sqrt{\pi}} + \frac{(1-\rho)^2}{2} + T\right] + \frac{m\sqrt{T}}{\rho\sqrt{\pi}} -$$

$$m\left(\frac{1}{\rho^2}\left(\frac{T}{4} + \frac{\sqrt{T}}{\sqrt{\pi}}\right)\right). \tag{A26}$$

The dimensionless current is

$$\mathrm{I} = \left[\frac{\partial V(\rho,T)}{\partial \rho}\right]_{\rho=1} = \frac{mT}{4} + \frac{mT-1}{2\sqrt{T}\sqrt{\pi}} - \frac{1}{2}. \tag{A27}$$

Edelweiss Applied Science and Technology
ISSN: 2576-8484
Vol. 9, No. 9: 1471-1483, 2025
DOI: 10.55214/2576-8484.v9i9.10155